Quantum Electronics **48** (8) 749–754 (2018) ©2018 Kvantovaya Elektronika and Turpion Ltd

https://doi.org/10.1070/QEL16675

Accounting for the instrument function of crystal spectrometers operating in many reflection orders in the diagnostics of laser plasma from its continuum spectrum

M.A. Alkhimova, I.Yu. Skobelev, A.Ya. Faenov, D.A. Arich, T.A. Pikuz, S.A. Pikuz

Abstract. **By the example of an X-ray spectrometer with a spherically bent mica crystal we consider the diagnostic errors entailed when the observed bremsstrahlung spectrum is attributed to a single spectrum of reflection. As an illustration we choose the X-ray emission spectrum of the plasma produced at the surface of a steel foil by femtosecond laser pulses of relativistic intensity. It is shown that obtaining adequate results in the case of a high-temperature plasma calls for the consistent inclusion of all orders of reflection or diffraction with a dispersing device.**

Keywords: *high-temperature plasma, X-ray spectroscopic diagnostics, crystal spectrometer, instrumental function.*

1. Introduction

A high-temperature plasma with an electron temperature $T_e \sim 100$ eV is a bright source of X-ray radiation. Since the characteristics of this radiation depend on plasma parameters, it would be natural to measure the emission spectra for diagnosing the plasma parameters. This line of investigation emerged back in the past century and is referred to as X-ray spectroscopic diagnostics of the plasma. Its importance was initially due to astrophysical requirements. Somewhat later the X-ray spectroscopic plasma diagnostics demonstrated its potentialities in the controlled thermonuclear fusion programmes, both magnetic- and inertial-confinement fusion, to become an integral part of these investigations (see, for instance, Refs [1–10]).

X-ray plasma radiation may be divided into line spectrum, which arises from bound–bound radiative transitions between the bound states of plasma ions, and continuous radiation, which arises either from the free–free transitions between the states of free plasma electrons (the bremsstrahlung) or from the free–bound transitions, i.e. the capture of free electrons to bound states (recombination radiation). The most abundant source of information about the plasma and the processes occurring in it is undoubtedly its X-ray line spectrum (see, for instance, Ref. [3]). However, in some cases the use of continuous emission spectra may be quite beneficial, which is stipulated by at least two reasons. First, the line spectrum may simply be absent in the case of the high-temperature plasma of light chemical elements, so that the continuous spectrum will be the only source of information. Second, extracting information from line spectra, as a rule, calls for rather complicated kinetic calculations, which cannot be sufficiently precise for all ions. By contrast, continuous spectra may be quite accurately described by simple universal formulas, so that the use a diagnostic technique reliant on the measurement of spectral characteristics is seemingly free from complications.

However, in reality some complications arise in this case, too. The point is that the crystals employed as dispersive elements of spectrometers (like diffraction gratings, though) quite frequently exhibit a high reflectivity in several order of reflection. For instance, the commonly used mica crystals exhibit a high reflectivity in the 1st, 2nd, 3rd, 5th, 8th, and 10th orders. As a result, recorded in experiment is the sum of emission spectra each of which corresponds to a certain order of reflection and consequently, to its own spectral range. When the line spectrum is recorded, the superposition of the orders is usually insignificant, because in most cases it is easily possible to ascribe a spectral line to one or other reflection order. The difficulty of ascribing to a certain order of reflection may arise, for instance, in the investigation of betatron plasma radiation [11]. When a continuous spectrum is recorded, as a rule it is the sum of the spectra of different orders, and it is impossible, strictly speaking, to separate out some single-order spectrum.

However, when use is made of the well-known method of determining plasma temperature from the shape of the bremsstrahlung or photorecombination spectrum, the observed spectrum is ascribed, as a rule, to only one order of reflection, neglecting the necessity of accounting for order summation. This approach is justifiable with the use of the photorecombination continuum when the recording range covers the domain near the ionisation potential of the corresponding ion whose position in the spectrum permits an unambiguous determination of the reflection order of the dispersing element that makes the main contribution to the spectrum under observation.

In our work we consider, by the example of an X-ray spectrometer with a spherically bent mica crystal [12–14], what diagnostic errors may be entailed when the observed bremsstrahlung spectrum is ascribed to a single reflection order. By way of illustration we take advantage of the previously

M.A. Alkhimova, I.Yu. Skobelev, D.A. Arich, S.A. Pikuz Joint Institute for High Temperatures, Russian Academy of Sciences, ul. Izhorskaya 13, stroenie 2, 125412 Moscow, Russia; National Research Nuclear University 'MEPhI', Kashirskoe sh. 31, 115409 Moscow, Russia; e-mail: spikuz@gmail.com;
A.Ya. Faenov Joint Institute for High Temperatures, Russian Academy of Sciences, ul. Izhorskaya 13, stroenie 2, 125412 Moscow, Russia; Open and Transdisciplinary Research Initiative, Osaka University, Osaka 565-0871, Japan;
T.A. Pikuz Joint Institute for High Temperatures, Russian Academy of Sciences, ul. Izhorskaya 13, stroenie 2, 125412 Moscow, Russia; Graduated School of Engineering, Osaka University, Osaka 565-0871, Japan

Received 12 March 2018; revision received 20 April 2018
Kvantovaya Elektronika **48** (8) 749–754 (2018)
Translated by E.N. Ragozin

obtained [15] X-ray emission spectra of the plasma produced by femtosecond laser pulses of relativistic intensity on the surface of a steel foil.

2. Relation between the recorded and emission spectra

Let a source radiate the spectrum $E(\lambda)$ and the detector record the spectrum $F(\lambda)$. If we use the wavelength scale corresponding to the mth reflection order for the spectrum $F(\lambda)$ observed on the detector and $S(\lambda)$ is the instrumental spectrometer function, we can write

$$F_m(\lambda_m) = \sum S\left(\frac{m\lambda_m}{n}\right)E\left(\frac{m\lambda_m}{n}\right), \quad (1)$$

where the sum in the right-hand side is taken over all significant reflection orders n.

Let us consider a continuous plasma emission spectrum. The functional wavelength dependences of the photorecombination $[E^{rc}(\lambda)]$ and bremsstrahlung $[E^{bs}(\lambda)]$ radiations are the same throughout the spectrum with the exception of the region near the ionisation threshold. So, when the photons with such near-threshold energies do not find their way to the recorded portion of the spectrum, it may be assumed that the intensity of the continuum is defined by the expression

$$E(\lambda) = E^{bs}(\lambda) + E^{rc}(\lambda) = A_0\lambda^{-2}\exp\left(-\frac{2\pi c\hbar}{\lambda k T_e}\right), \quad (2)$$

where the constant A_0 characterises the total intensity of the continuum. Substitution of expression (2) in formula (1) permits calculating the continuous spectrum recorded from the plasma with a temperature T_e and selecting the temperature and the normalisation constant A_0 that best describe the spectrum observed.

Since the observed spectrum is obtained from the emission one by multiplying it by the instrumental function and summing over the orders of reflection, these spectra, generally speaking, will have different shapes. The inclusion of instrumental function is a standard well-known procedure when the observed spectrum is due to only one order of reflection. In this case it is possible either to divide the observed spectrum by the instrumental function of known order and thereby recover the emission spectrum to subsequently compare it with the model one, or to multiply the model spectrum by the instrumental function and compare it with the observed one. When the dispersing element operates by several orders of reflection (or diffraction), the former approach cannot be applied. In this case, the model spectrum has to be multiplied by the instrumental function of the corresponding order of reflection, the results should be summed for all orders, and the resultant spectrum should be compared with the observed spectrum.

In the general case, the instrumental function $S(\lambda)$ of a spectrometer may be split into the factors describing the dispersing element efficiency (the reflection coefficient) $R(\lambda)$, the transmittance $T(\lambda)$ of the filters in use, and the detector efficiency $D(\lambda)$:

$$S(\lambda) = R(\lambda)T(\lambda)D(\lambda). \quad (3)$$

Since the further consideration calls for concretisation of the spectrometer instrumental function, we perform it without loss of generality by the example of a spectrometer with a spherically bent mica crystal, which was employed in our investigation [15] of the emission spectra of the laser-produced plasma of thin steel foils. Figure 1 shows the X-ray spectroscopic complex used in this experiment. It comprises a focusing spectrometer with spatial resolution (FSSR) equipped with a spherically bent mica crystal (radius of curvature: 150 mm; interplanar spacing $2d = 19.94$ Å), an Andor DX-434 CCD camera (detector pixel size: 13.5 μm) for an X-ray detector, as well as a set of filters used to protect the detector from illumination by optical radiation and prevent the dispersing element from being coated.

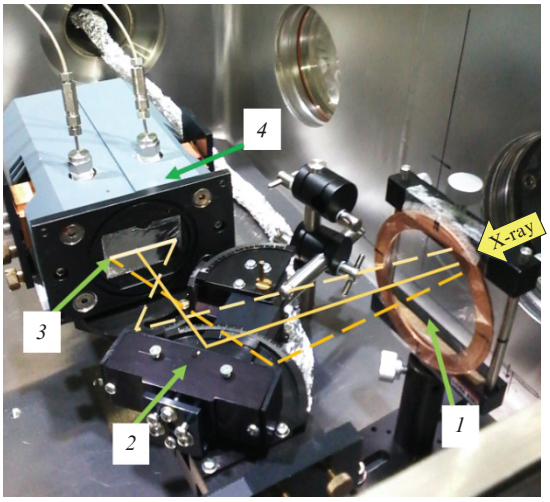

Figure 1. X-ray spectroscopic complex employed in Ref. [15]: (*1*) Mylar filter; (*2*) spherically bent crystal; (*3*) filters in front of the CCD detector matrix; (*4*) Andor CCD detector.

To reduce the contribution of the noise signal caused by the high-energy electrons from the plasma, placed in front of the X-ray spectroscopic complex were permanent magnets (NeFeB) with $B \approx 0.5$ T, which formed a diagnostic window 15 mm in diameter. The X-ray radiation transmitted through the diagnostic window was attenuated with a Mylar filter (filter f1 in what follows) placed in front of the crystal to protect the reflecting surface from being coated. The filter thickness was selected depending on the experimental conditions: used most often was a thin ($h = 10$ μm) or thick ($h = 100$ μm) Mylar filter. The matrix of the X-ray CCD camera was shielded from visible light by two 1-μm thick polypropylene film layers coated with aluminium of thickness 0.2 μm (filter f2). It is noteworthy that the transmittance of the aluminium layer, as shown in Ref. [16], is significantly changed when the filter is irradiated by high-power laser radiation, which should undoubtedly be taken into account.

The dispersing element of the spectrometer was oriented so as to observe the spectrum in the wavelength range 1.6–2.1 Å in the 8th reflection order. This range contains the spectral lines of iron ions arising from transitions to the K shell (from the Ly_α line of hydrogen-like Fe XXVI ions to the K_α line of neutral iron). Some lines of chromium ions also fall into this range. Since mica crystals possess a rather high reflectivity in the orders specified above [11], the radiation from all spectral regions indicated in Table 1 found its way to the spectrum observed. The contribution from each reflection order to the overall observed spectrum is defined by its weight factor $S(\lambda)$,

Table 1. Recorded spectral ranges.

Reflection order	Wavelength range/Å	Reflection order	Wavelength range/Å
1	13.2–16.4	5	2.64–3.28
2	6.6–8.2	8	1.65–2.05
3	4.4–5.46	10	1.35–1.64

which is the instrumental function in a given reflection order calculated by formula (3). We note that the reflection order which contains the line spectra is convenient to adopt for a 'reference' order m used to construct the wavelength scale. Below we therefore assume that $m = 8$.

The factors defining the instrumental function of our X-ray spectroscopic complex in different orders of reflection are plotted as functions of the wavelength λ_m in Fig. 2. The transmittances of different filters were calculated by an open access program [17].

Note that the reflection properties of mica have not been studied experimentally in sufficient detail, because each crystal should by studied separately due to its complex mosaic structure and the lattice deformation due to its bending. The data on reflectivity curve measurements for spherically bent mica crystals are outlined in Refs [18–21], but these data are insufficient for considering the efficiency of reflection by the crystal for a large number of reflection orders. That is why the reflectivity of the mica crystal in each of the orders under consideration was obtained with the use of the data of Ref. [22] in the framework of general diffraction theory for a plane mica crystal.

The CCD detector efficiency $D(\lambda)$ depends on the quantum efficiency $Q(\lambda_m)$ of its matrix [23] specified, as a rule, in the device certificate and on the incident photon energy: $D(\lambda) \sim \hbar\omega_m Q(\lambda_m) \sim Q(\lambda_m)/\lambda_m$. Although the quantum efficiency for shorter-wavelength photons is not very high (~10%–15%), these photons most efficiently produce electron–hole pairs. As a result, the recording efficiency for the radiation corresponding to the 3rd, 5th, and 8th reflection orders turns out by be appreciably higher than for the 1st, 2nd, and 10th orders (see Fig. 2c).

In our experiments use was made of filter f1, which was a 10- or 100-μm thick Mylar film, and so Fig. 3 shows the resultant instrumental functions for these two cases.

As is clear from Fig. 3, the efficiency of recording the spectral ranges corresponding to the 1st and 2nd orders of reflection is very low, while the values of the instrumental function in the 3rd–10th orders are quite comparable. Knowing the instrumental function, it is easy to determine the contribution of different orders of reflection to the recorded spectrum. For instance, plotted in Fig. 4 for the bremsstrahlung emission spectra $E(\lambda)$ described by formula (2) at temperatures of 100, 500, 1000, and 2000 eV are their corresponding observed spectra $F_8(\lambda_8)$ calculated with and without the inclusion of summation over reflection orders. Also shown here are the contributions of the reflection orders for different filter thicknesses for the X-ray spectroscopic complex under consideration.

Several conclusions may be drawn from the curves plotted in Fig. 4. First of all, it is evident that the observed continuous

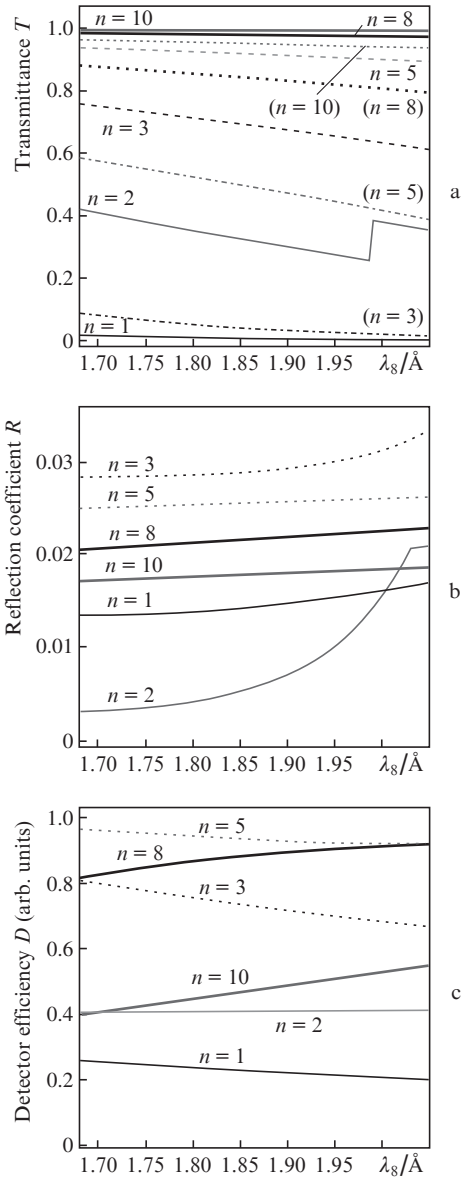

Figure 2. (a) Filter transmittances T, (b) mica reflection coefficients R, and (c) detector efficiency D in relation to the wavelength λ_8 for different orders of reflection. The data plotted in Fig. 2a were obtained for an f1 filter thickness of 10 (solid and dashed lines) and 100 μm (dotted and dash-dotted lines).

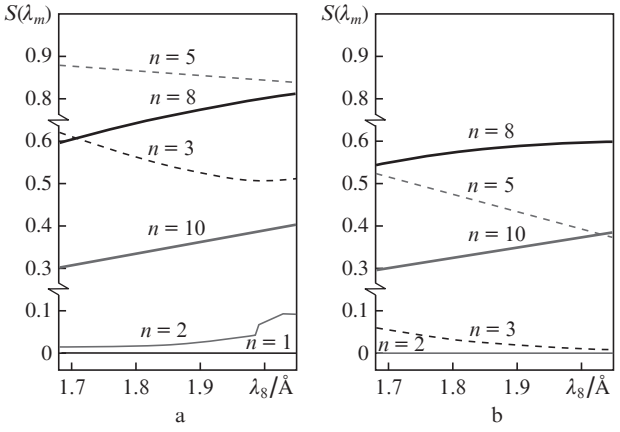

Figure 3. Instrumental function $S(\lambda)$ of the X-ray spectroscopic complex in relation to the wavelength λ_8 when use is made of (a) 10- or (b) 100-μm thick Mylar film as the f1 filter.

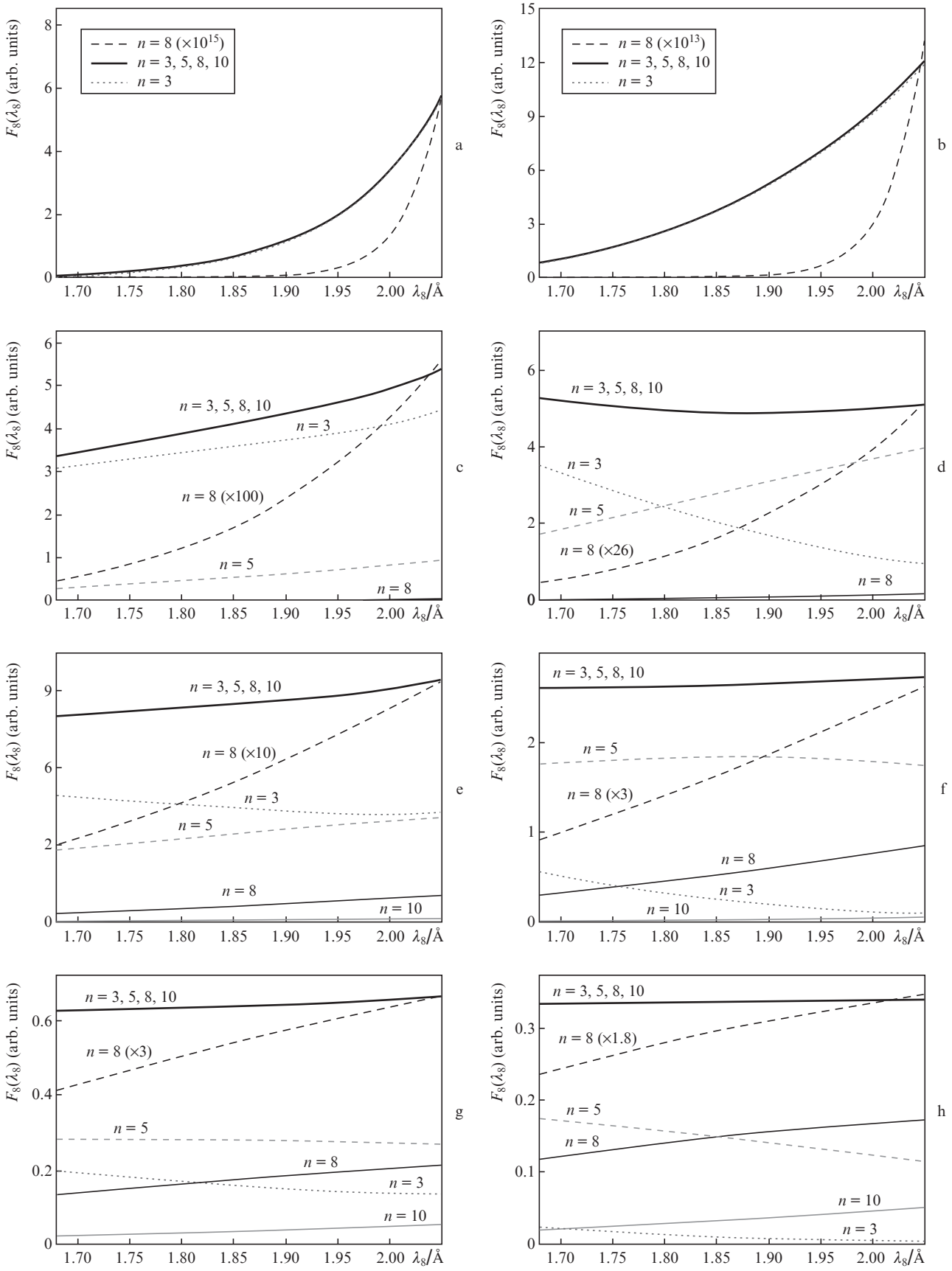

Figure 4. Observed $F_8(\lambda_8)$ spectra calculated for bremsstrahlung $E(\lambda)$ spectra with temperatures of (a, b) 100, (c, d) 500, (e, f) 100, and (g, h) 2000 eV with the inclusion of summation over reflection orders for 10- (at the left) and 100-μm (at the right) thick filters. The dashed curves show the contribution of the 8th order of reflection normalised to the total spectrum at the point with a wavelength of 2.08 Å (shown in parentheses is the scaling factor for a given plot).

spectrum is due to one order of reflection only at low plasma temperatures. With increasing temperature to ~500 eV the higher-order contributions may no longer be neglected, especially when use is made of additional filters. We emphasise: when the observed spectrum is ascribed to a single reflection order, quite incorrect inferences may be drawn about the plasma temperature. As shown in Fig. 4 with dashed lines, ascribing the spectrum, for instance, to the 8th order results in a quite incorrect description of the observed spectrum.

Another important conclusion is that the inclusion of several orders of reflection lowers the sensitivity of the shape of the observed spectrum to the temperature (the spectrum becomes flatter), which naturally limits the diagnostic potentiality of the method, especially in the high-temperature domain. An evident way of broadening the diagnostic interval towards higher temperatures involves the use of additional filters to radically suppress the low-order recording efficiency.

3. Comparison with experiment

The experiments to investigate the X-ray emission from steel foils were carried out on the J-KAREN-P laser facility (Kansai Photon Science Institute, Japan) in Ref. [15]. A laser pulse with a duration $\tau \approx 40$ fs (FWHM) and a wavelength $\lambda = 0.8$ μm was focused on the surface of a thin steel foil at an angle of 45° to the target surface to a spot with diameter $d \approx 2$ μm. The laser pulse energy E_{lt} at the target amounted to ~10 J and the peak intensity I_{lt} ranged up to $\sim 3.2\times10^{21}$ W cm^{-2}. For a target use was made of a stainless steel tape (AISI304: 72% Fe, 18% Cr, 10% Ni) of thickness $h = 5$ μm. The FSSR X-ray spectrometer with a resolving power $\lambda/\Delta\lambda \sim 3000$ was positioned for observing the spectra from the front foil surface at an angle of about 8° to the normal to the target surface.

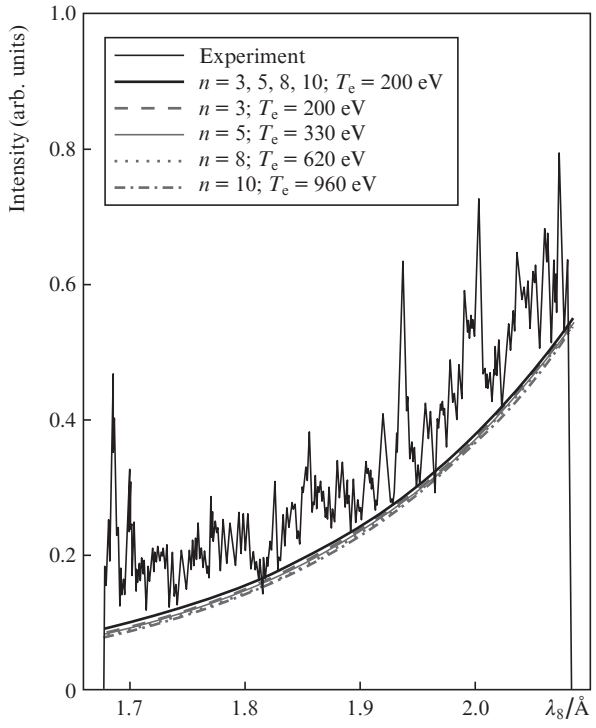

Figure 5. Emission spectrum of the steel plasma recorded with the 10-μm thick Mylar filter in Ref. [15]. Shown are the approximations of the spectrum with the inclusion of a single order of reflection, and their corresponding plasma temperatures are given.

Figure 5 shows the spectrum recorded with the use of the thin Mylar filter. With the inclusion of all orders of reflection, the continuous component of the spectrum is nicely described by a temperature of 200 eV. Simulations suggest in this case that the 3rd order of reflection makes the main contribution to the observed continuous spectrum, although the line component corresponds to the 8th order. If this spectrum is ascribed to another order of reflection, it can be nearly equally well described by model curves, though at quite incorrect temperature values equal to 330 eV (for the 5th order), 620 eV (for the 8th order), and 960 eV (for the 10th order).

4. Conclusions

In this work we analysed how the inclusion of different reflection orders of the dispersing device affects the plasma diagnostics from the shape of continuous radiation. It was shown that the inclusion of several reflection orders, generally speaking, lowers the sensitivity of the observed spectrum to the temperature, thereby limiting the diagnostic potentialities of the method. This effect is most pronounced at a high plasma temperature. An efficient way of broadening the diagnostic interval towards higher temperatures involves the use of additional filters that reduce the low-order recording efficiency.

As shown in our work, in the heating of a thin steel foil by femtosecond laser pulses of relativistic intensity the spectrum recorded with a mica crystal spectrometer corresponds to an electron temperature of 200 eV, while the inclusion of only one reflection order in the interpretation of the spectrum permits obtaining practically any temperature value in the 200–960 eV range. Our results allow a conclusion to be made that the high-temperature plasma diagnostics from the shape of continuous spectrum calls for the consistent inclusion of all orders of reflection or diffraction with a dispersing device.

Acknowledgements. This work was performed at the Joint Institute for High Temperatures of the Russian Academy of Sciences under financial support of the Russian Science Foundation (Grant No. 17-72-20272).

References

1. Lochte-Holtgreven W. (Ed.) *X-Ray Diagnostics of Plasmas* (New York: American Elsevier, 1968; Moscow: Mir, 1971).
2. Luk'yanov S.Yu. *Goryachaya plazma i upravlyaemyi yadernyi sintez* (Hot Plasma and Controlled Nuclear Fusion) (Moscow: Nauka, 1975).
3. Boiko V.A., Vinogradov A.V., Pikuz S.A., Skobelev I.Yu., Faenov A.Ya. *Itogi Nauki i Tekhniki. Ser. Radiotekh.*, **27**, 171 (1980).
4. Basov N.G., Zakharenkov Yu.A., Rupasov A.A., Sklizkov G.V., Shikanov A.S. *Diagnostika plotnoi plazmy* (Dense Plasma Diagnostics) (Moscow: Nauka, 1989).
5. Gavrilenko V.P., Faenov A.Ya., Magunov A.I., et al. *Phys. Rev. A*, **73**, 013203 (2006).
6. Faenov A.Ya., Skobelev I.Yu., Pikuz T.A., et al. *Pis'ma Zh. Eksp. Teor. Fiz.*, **94**, 187 (2011).
7. Skobelev I.Yu., Faenov A.Ya., Pikuz T.A., Fortov V.E. *Phys. Usp.*, **55**, 47 (2012) [*Usp. Fiz. Nauk*, **182**, 49 (2012)].
8. Albertazzi B., Ciardi A., Nakatsutsumi M., et al. *Science*, **346**, 325 (2014).
9. Faenov A.Ya., Oks E., Dalimier E., et al. *Quantum Electron.*, **46**, 338 (2016) [*Kvantovaya Elektron.*, **46**, 338 (2016)].
10. Revet G., Chen S.N., Bonito R., et al. *Sci. Adv.*, **3**, e1700982 (2017).

11. Andreev A.A., Platonov K.Yu. *Quantum Electron*., **46**, 109 (2016) [*Kvantovaya Elektron*., **46**, 109 (2016)].
12. Faenov A.Y., Pikuz S.A., Erco A.I., et al. *Phys. Scr*., **50**, 333 (1994).
13. Skobelev I.Yu., Faenov A.Ya., Bryunetkin B.A., et al. *Zh. Eksp. Teor. Fiz*., **108**, 1263 (1995) [*JETP*, **81**, 692 (1995)].
14. Lavrinenko Ya.S., Morozov I.V., Pikuz S.A., Skobelev I.Yu. *J. Phys.: Conf. Ser*., **653**, 12027 (2015).
15. Faenov A.Ya., Alkhimova M.A., Pikuz T.A., et al. *Appl. Phys. B*, **123**, 197 (2017).
16. Bykovskii N.E., Pershin S.M., Samokhin A.A., Senatskii Yu.V. *Quantum Electron*., **46**, 128 (2016) [*Kvantovaya Elektron*., **46**, 128 (2016)].
17. http://henke.lbl.gov/optical_constants/.
18. Pikuz T.A., Faenov A.Ya., Pikuz S.A., et al. *J. X-Ray Sci. Technol*., **5**, 323 (1995).
19. Monot P., Auguste T., Dobosz S., et al. *Nucl. Instrum. Methods Phys. Res., Sect. A*, **484**, 299 (2002).
20. Sanchez del Rio M., Alianelli L., Pikuz T.A., et al. *Rev. Sci. Instr*., **72**, 3291 (2001).
21. Alkhimova M.A., Pikuz S.A., Faenov A.Ya., et al. *J. Phys.: Conf. Ser*., **774**, 012115 (2016).
22. Henke B.L., Jaanimagi P.A. *Rev. Sci. Instr*., **56**, 1537 (1985).
23. http://www.andor.com.